We thank the reviewers for their thoughtful comments. Our responses to each of the major and minor comments are provided below. The text in normal font is our direct response to the reviewer and the text in italic font is the text that are added/edited in the manuscript.

Reviewer 1 response:

Major Comments:

1. **Lookup Table (Lines 161-162): The lookup-table data has not been provided anywhere. I would suggest including them as a part of publicly available data, so that someone interested in reproducing/verification by independent means can use/validate them.**

   The lookup table is provided as part of the publicly available data for reproducibility and verification as described in the Data Availability section. Note that the lookup table is dependent on instrument performance so the provided table is most appropriately used for the November 2-8, 2018 period where we have quantified GOLD's performance (wavelength resolution and registration variations along the detector). We cannot guarantee accurate temperatures outside of this period.

2. **PCA of simulated LBH emissions: Line 115: "The second leading....(.. explained later)". This is not clear to me how the 2nd leading mode would only contain the temperature variability. Why would it not contain, for example, the geomagnetic. variability? Can you use a bunch of simulated spectra corresponding to temperatures in the 300-1500 Kelvin range and show that the 2nd leading mode is associated only with temperature changes?**

   The modes of variability derived from data via PCA decompose the variability in data into orthogonal directions that are not necessarily associated with a particular geophysical source of variability. The shape of the second mode suggests that it is capturing the broadening of individual LBH bands that can only be attributed to changes in the rotational temperature of N_2. Using the associated coefficients to the modes of variability, we can investigate how the variability in data at a specific time and location can be projected into each mode to gain insight into the source (geomagnetic activity, SZA, OZA, etc.).

   In the case of increased geomagnetic activity, for example, we see coefficients associated with the first mode of variability increase particularly in the high latitudes as there is more excitation of LBH emissions. At the same time, we see the coefficients associated with second mode increase as temperatures rise and the LBH bands broaden.

The following text is added to the beginning of Section 2.2 (Lines 94-107) to help clarify the meaning of the PCA results.

"*PCA is a data reduction technique that is useful for identifying the dominant orthogonal modes of variability from data. PCA is applied here using eigenvalue decomposition of a sample covariance matrix,* $\boldsymbol{S}_{\lambda\lambda}$*, of simulated LBH emissions,* $\boldsymbol{I}^{s}_{LBH}$*, at wavelengths,* $\boldsymbol{\lambda}$*, is computed from aggregated data sets of simulated emissions of the LBH band system during 2–8 November 2018 for a total of N = 8.1×10*^{4} *samples.*

$$\boldsymbol{S}_{\lambda\lambda} = \frac{1}{N-1}\sum_{i=1}^{N} {\boldsymbol{I}^{s\prime}_{LBH_i}}^{T} \boldsymbol{I}^{s\prime}_{LBH_i}$$

$$\boldsymbol{I}^{s\prime}_{LBH_i} = \boldsymbol{I}^{s}_{LBH_i} - \overline{\boldsymbol{I}^{s}_{LBH}}$$

$\overline{\boldsymbol{I}^{s}_{LBH}}$ *is the mean LBH spectrum of the N samples. The useful results of PCA for this investigation are a set of eigenvectors (principal components),* **v***, that describe the mode of variability in the LBH band system***,** *with associated eigenvalues,* σ*. Suppose that* **v** *is an orthonormal set of spatiotemporally invariant basis and spatiotemporal dependent coefficients,* **c***, represent the amplitude of the mode for each disk emission sample at a given time,* t_i*, and location,* r_i*, then* $\boldsymbol{I}^{s\prime}_{LBH}$ *can be expressed:*

$$\boldsymbol{I}^{s\prime}_{LBH_i}(\boldsymbol{\lambda}, r_i, t) = c_1(r_i, t_i)\,\boldsymbol{v}_1(\boldsymbol{\lambda}) + c_2(r_i, t_i)\,\boldsymbol{v}_2(\boldsymbol{\lambda}) + \ldots + c_n(r_i, t_i)\,\boldsymbol{v}_n(\boldsymbol{\lambda}) + \boldsymbol{d}'(\boldsymbol{\lambda}, r_i, t_i)$$

where $\boldsymbol{d}'(\boldsymbol{\lambda}, \boldsymbol{r}, t)$ *is the residual after subtracting the mean and the sum of n weighted modes from* $\boldsymbol{I}^{s}_{LBH_i}$*. The total variance of* **c** *matches* σ^2 *for that mode.* "

In addition to this added text, Figure 2 is updated to further illustrate the meaning of the second mode of variability.

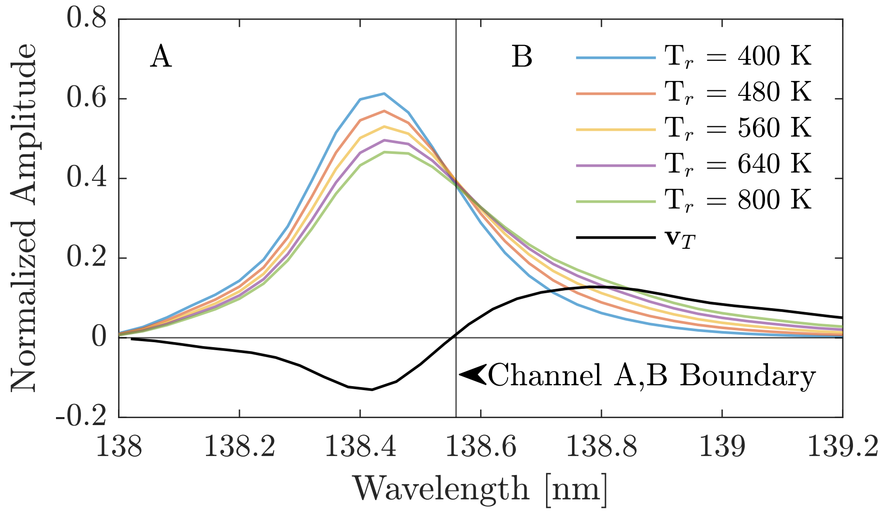

Figure 2: The second principal component (black line), v_T, over the LBH (2,0) band and the normalized amplitude of the LBH (2,0) band at six N_2 rotational temperatures, T_r. Emissions at 138.56 nm, where v_T changes the sign, are independent of temperature, and provide a boundary location to divide the (2,0) band into channels A and B.

3. **Shot noise: It is said that the spectra are just simulated/model/synthetic spectra. How can a model/simulated spectra will contain shot noise? Are you using a set of spectra or introducing some random noise in the spectra and then calculating the shot noise? Please add more explanations.**

   The reviewer makes a good point. In defining the shot noise amplitude in Section 2.2 to compare against the second mode, we simply took the square root of the mean brightness in Rayleighs of each spectral bin of the (2,0) band. This is incorrect as shot noise is instrument specific and should be run through an instrument simulator. In addition to this point, we have determined that it is not appropriate to use the principal component analysis results to quantify signal-to-noise ratio as the modes of variability and associated coefficients do not provide total signal amplitude at a given time and location, only deviations in signal amplitude from the mean.

   For these reasons, we have removed all text associated with quantifying the temperature signal-to-noise in Section 2.2. We have also removed the shot noise amplitude in Figure 2 (shown above). Removing this text does not change the major results of this manuscript.

4. **Variation in wavelength registration: Better used an atomic line but try to avoid OI-135.6 nm as it is very strong emission and on occasions degrades**

the detector. Variation in wavelength resolution: Again, better try to use some atomic line other than OI-135.6 nm.

With the understanding that the GOLD team is using atomic lines for both wavelength registration and resolution estimates, we argue that while wavelength resolution estimates likely need an atomic line to prevent the rotational structure of a molecular band interfering with the estimate of the width of the feature, estimates of wavelength registration do not need an atomic line. This is because wavelength registration is estimated with the location of the peak of the band (in this case (2,0) band) where this peak does not vary with the rotational structure of the band. However, this peak does vary with the wavelength resolution, so the resolution must first be estimated before fitting the (2,0) band to estimate the registration. This procedure is used in the manuscript.

The text is updated as follows (Lines 247-250):

"*Variations in wavelength resolution along the GOLD detector are identified with the FWHM of the OI 135.6 doublet through fitting a 2-gaussian distribution. Variations in the wavelength registration are identified by differencing the modeled peak wavelength given the fitted OI 135.6 doublet FWHM by the peak wavelength determined by fitting a log-normal distribution to the (2,0) band. Note that the degradation of the detector due to the strength of the OI 135.6 doublet can cause errors in the spectral resolution estimate, but significant degradation had not occurred by 2-8 November 2018.*"

5. **GOLD case study: Why you are not using the errors available in the L1C data? Why do you need to simulate the error?**

   We are using the errors in photon counts provided in the L1C data to simulate errors in temperature.

   The text is updated as follows (Lines 169-171):

   "*The T_{ci} random measurement error given the random error in photon counts provided in the GOLD L1C data is quantified using Monte Carlo (MC) samples of simulated T_{ci} derivations considering the viewing conditions and instrument performance (McClintock et al., 2020a,b).*"

6. **"T_{ci}^{G} is also….based on the SZA." In the previous section it is stated that sampling at peak altitudes introduces 30-90K error. Then why are you using MSIS sampled at peak altitudes. I would recommend calculating**

GOLD equivalent effective temperatures using MSIS profiles and contribution functions from radiative transfer model. It will give better comparison with GOLD L2-Tdisk, particularly with version 3 TDISK. This can be presented as an additional row in the comparison (Figure 5).

For the comparison to MSIS in Section 4, we do not sample MSIS at the peak of the contribution function, $p_{\tau=1}$, (red points in Figure 6) for the given SZA but instead at the pressure with the temperature that most closely matches the derived temperature based on simulated derivations, $p_{T_{ci}^{s}}$, (black points in Figure 6).

While responding to the reviewer's comment, we realized that the contribution function is not only dependent on SZA but also on OZA. The sampling of MSIS thus should consider the SZA and OZA. The following figure is added to Section 3.3.

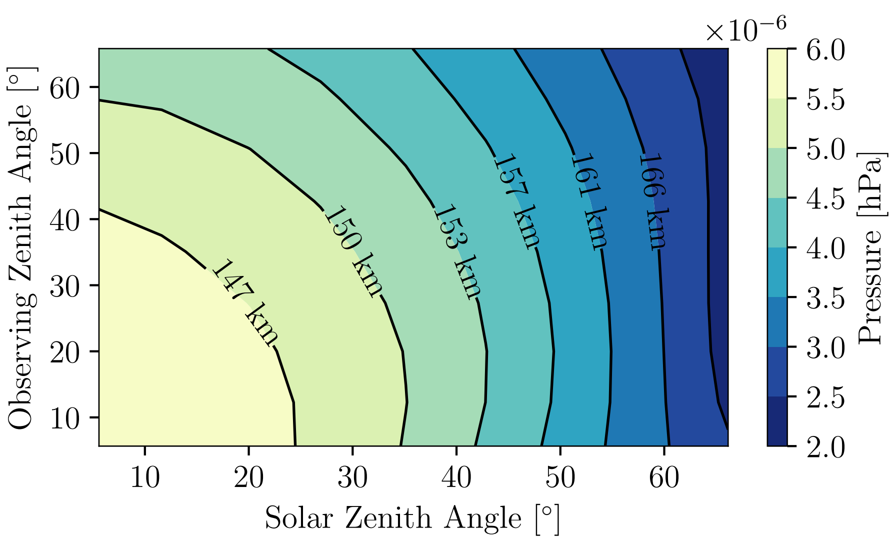

Figure 5: Pressure at the peak of the LBH contribution function, $p_{\tau=1}$, as a function of SZA and OZA determined from forward modeling WAM simulations for the period of November 2-8, 2018 considering realistic forcing conditions. LBH emissions are on constant pressure level surfaces given the solar and observing zenith angles. Approximate corresponding altitudes in the WAM simulations are also provided but note that these altitudes would vary depending on the forcing conditions.

Text corresponding to the new Figure 5 is added in Section 3.3 as follows (Lines 202-204):

"The LBH contribution function peak, $p_{\tau=1}$, changes with solar zenith angle (SZA) and observing zenith angle (OZA) as shown in Fig. 5. $p_{\tau=1}$ decreases in pressure (increases in altitude) for increases in SZA and OZA with a stronger dependence on SZA."

Based on the information summarized in this new figure, we have remade Figure 4 (now Figure 6), removing the OZA dependence and plotting in terms of pressure.

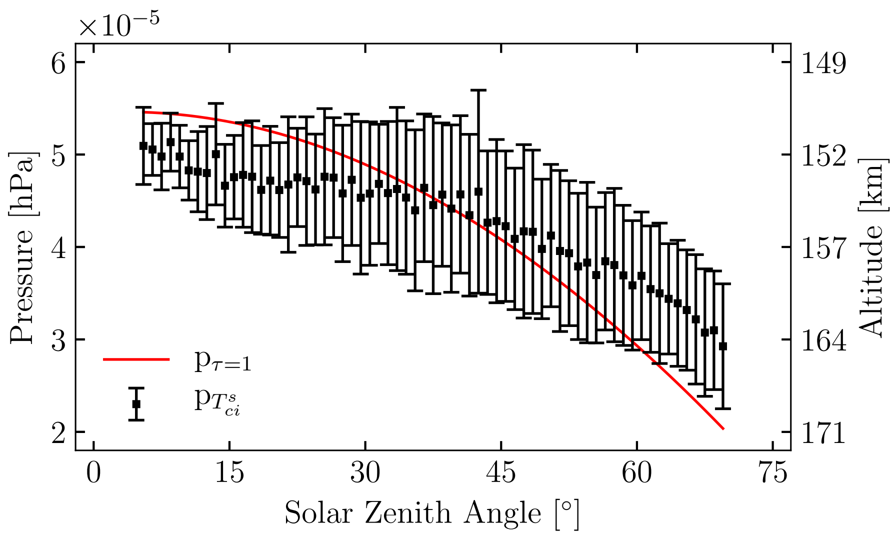

Figure 6: The mean and standard deviation of the pressure for the simulated WAM temperature that is closest to T^s_{ci} , $p_{T^s_{ci}}$, as a function of SZA averaged over all OZA for the simulation period of 2–8 November 2018 (black). The peak of the LBH contribution function, $p_{\tau=1}$, is shown as a function of SZA based on forward modeling of LBH disk emissions using the same WAM simulation (red). This peak is constant with respect to pressure level for a given SZA. The approximate altitudes for the pressures are also provided.

The conclusions that can be drawn from the updated Figure 6 remain the same in that the derived temperature is a column-integrated quantity and should not be attributed to the altitude of the peak of the contribution function. However, the interpretation of Figure 4 in Section 3.3 has been updated. Updates include changing $z_{\tau=1}$ to pressure level, $p_{\tau=1}$, and $z_{T^s_{ci}}$ to pressure level, $p_{T^s_{ci}}$. The text in Section 3.3 is updated as follows (Lines 204-213):

"Removing the OZA dependence, Fig. 6 shows there is a clear difference in $p_{\tau=1}$ and $p_{T^s_{ci}}$ in their respective dependences on SZA ($p_{T^s_{ci}}$ ranges 3×10^{-5} – 5×10^{-5} hPa and $p_{\tau=1}$ ranges 2×10^{-5}– 5.5×10^{-5} when SZA ranges 5º–70º). The weaker SZA

dependence of $p_{T^s_{ci}}$ can be explained by the FWHM of the contribution function that spans ~60 km at low SZA and ~90 km for high SZA (Laskar et al., 2020). The contribution function acts as an averaging kernel for temperature over these large vertical widths that tends to reduce the SZA effect. The net result is derived temperatures that are generally hotter than temperatures at $p_{\tau=1}$ ($p_{T^s_{ci}} < p_{\tau=1}$) for low SZA and temperatures that are generally cooler than temperatures at $p_{\tau=1}$ ($p_{T^s_{ci}} > p_{\tau=1}$) for high SZA. Figure 6 also shows variability in $p_{T^s_{ci}}$ (up to 1.5×10^{-5} hPa or ~10 km for the simulation conditions) at a given SZA that reflects considerable variability in the vertical temperature structure within the width of the contribution function given varying forcing conditions."

Finally, the T_{MSIS} temperatures have been updated with altitude sampling as a function of both OZA and SZA instead of just SZA like initially performed. This updated sampling results in cooler T_{MSIS} temperatures such that there is now the best agreement between T^G_{ci} and T_{DISK}. The interpretation of Figure 5 (now Figure 7) is updated in the manuscript. This update does not affect the major conclusions in the manuscript.

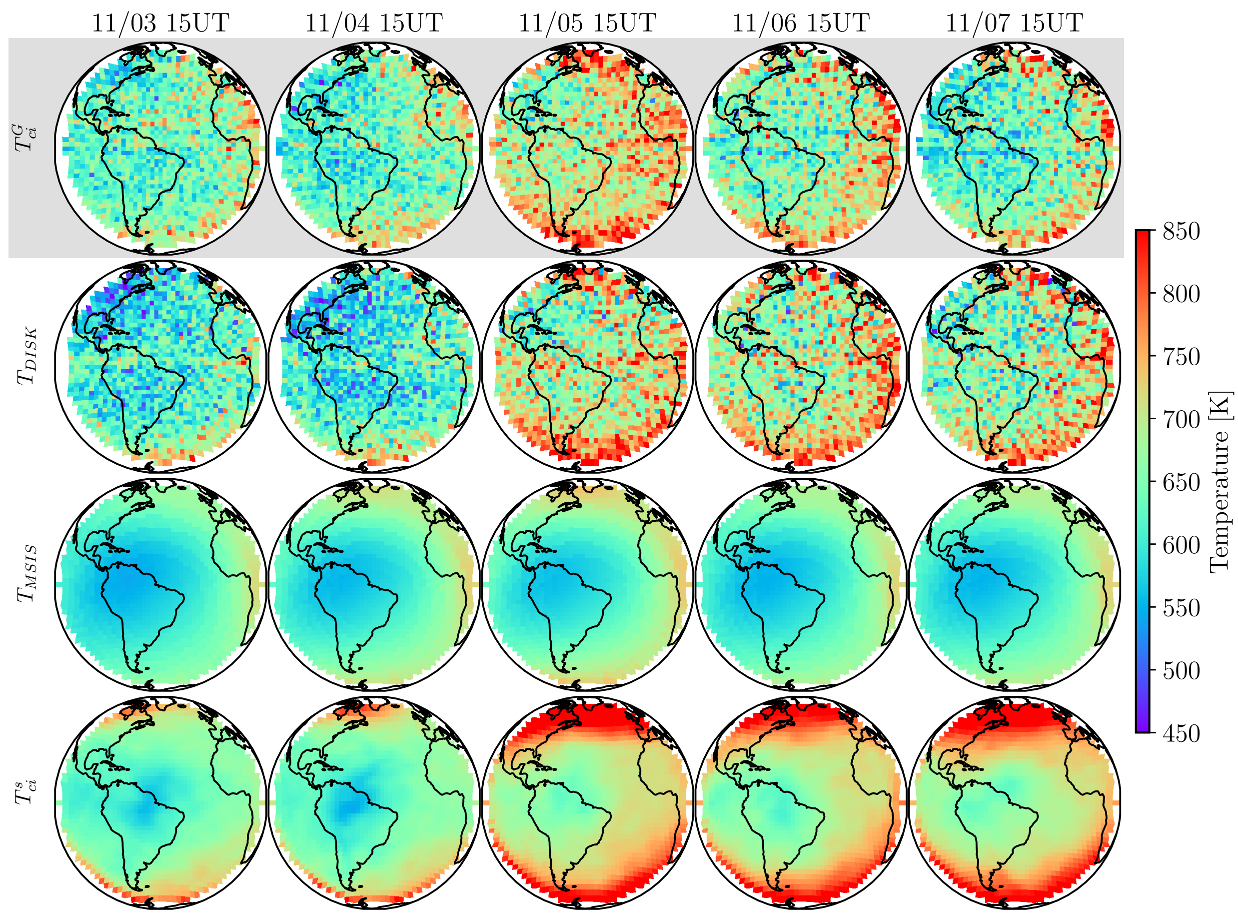

Figure 7: Comparison of T_{ci}^{G} with T_{DISK}, T_{MSIS}, and T_{ci}^{s} over Earth's disk viewed by GOLD for a five-day window from 3-7 November 2018 at about 15 UT, noon LT at the center of the disk (47.5°W, 0°N). A small geomagnetic storm has commenced the evening of 4 November and lasted through 5 November.

7. **Section 4: The authors used the unbinned data from an old release version-2 (V2), which I cannot locate in the two GOLD repositories provided in the data availability section. As there is poor signal to noise (SNR) concern and potential bias concern, I would suggest revising the analysis and results with version 3 (V03) GOLD TDISK and 2x2 binned L1C data (L1C-V03). Specifically, revise Figure 5 with the V03 data.**

   The analyses have been revisited with version 3 of the GOLD TDISK data that use binned L1C data. Figures 5 and 6 (now Figures 7 and 8) have been updated with the version 3 data. There are no major changes to results associated with updating to version 3, but there is in general better agreement between T^{G}_{ci} and TDISK in Figures 7 (see response to Major Comment 6) and 8. However, a deeper comparison between T^{G}_{ci} and TDISK version 3 as a function of SZA and OZA shows systematic differences between these datasets as discussed as part of the response to Major Comment 8.

8. **Previously the authors mentioned that this retrieval is unaffected by biases in emission intensities as the absolute values are not important, but the spectral shapes are. Then why would systematic errors in intensities, which will basically introduce some bias, would introduce bias in temperature calculation? This also contradict the conclusions in lines 318-322, which says absolute band intensities are not required.**

   The systematic errors arise from wavelength registration and resolution errors which changes the <u>relative</u> magnitude of each channel and ultimately the resulting temperature. We have been able to significantly (although not completely) reduce the systematic errors in temperature arising from GOLD wavelength registration and resolution errors using the procedure described in Major Comment 4.

   This procedure only requires <u>relative</u> magnitudes in each channel and not radiometrically calibrated absolute intensities. This is a major motivation for the procedure that considerably simplifies the forward model (and associated errors) from a forward model that would need an airglow volume emission rate model like GLOW and a radiative transfer model to determine absolute intensities to a forward model that only consists of the LBH rotational vibrational band model to determine relative magnitudes in each channel for a given temperature.

Further comparisons between T^G_{ci} and TDISK were performed to assess biases in the temperatures that are attributable to differences in the retrieval techniques. The following new figure and text has been added to Section 4.2 as follows (Lines 276-296).

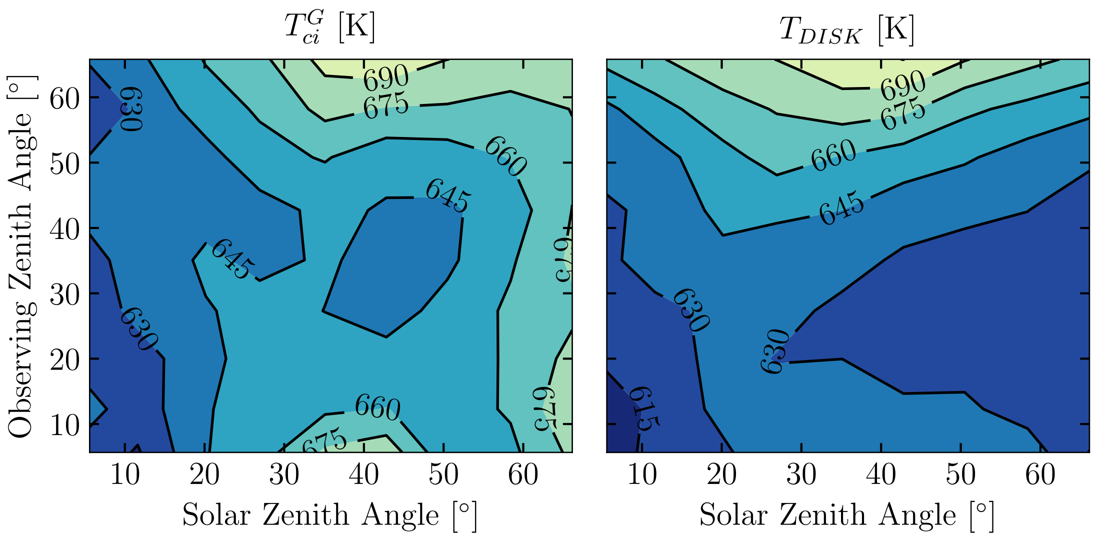

Figure 9: Mean T^G_{ci} and T_{DISK} temperatures as a function of SZA and OZA for the period of 2–8 November 2018 with 5º binning in SZA and OZA.

"The T^G_{ci} and T_{DISK} comparison is expanded in Fig. 9 to include all times in the range 7–22 UT for the period of 2–8 November 2018. It is clear in Fig. 9 that T^G_{ci} and T_{DISK} have very different dependencies on the viewing conditions determined by SZA and OZA. T^G_{ci} increases with both SZA and OZA with a stronger dependence on SZA. T_{DISK} increases with OZA but remains relatively uniform with SZA even decreasing slightly for SZA > 25º. There are two likely explanations for the dependence of the derived temperature on viewing conditions: (1) The derived temperatures reflect real temperature changes with viewing conditions because of the contribution function peaking at different pressures (Fig. 5). (2) The derived temperatures reflect temperature biases with viewing conditions because of changes in the LBH emission intensity. Intensity decreases with increasing SZA due to reduced LBH excitation but increases with increasing OZA due to a larger airmass along the line-of-sight. To test which explanation best describes the dependence of T^G_{ci} and T_{DISK} on viewing conditions, Fig. 9 is correlated to the pressure at the peak of the LBH contribution

function, $p_{\tau=1}$, (Fig. 5) and to the mean LBH intensity measured by GOLD over the same period as a function of SZA and OZA. T_{DISK} is weakly correlated (R=-0.15) with $p_{\tau=1}$ and strongly correlated (R=0.72) with LBH intensity. In contrast, T_{ci}^{G} is strongly correlated (R=-0.86) with $p_{\tau=1}$ and weak-moderately correlated (R=-0.32) with LBH intensity. The stronger correlation between T_{ci}^{G} and $p_{\tau=1}$ compared to T_{DISK} and $p_{\tau=1}$ and weaker correlation between T_{ci}^{G} and LBH intensity compared to T_{DISK} and LBH intensity over this analysis period is suggestive that T_{ci}^{G} is more sensitive to real temperature changes as the probed pressures change with viewing conditions and less susceptible to biases due to a change in LBH intensity with viewing conditions. This is attributed to the fact that T_{ci}^{G} derivation does not require measurement of a fully resolved, radiometrically calibrated LBH band system nor a forward model to produce absolute LBH intensity. There is likely still biases in T_{ci}^{G} with LBH intensity as indicated by the weak-moderate correlation (R=-0.32), particularly at low intensities (high SZA) where shot noise can lead to positive biases up to 15 K in the two-channel ratio approach."

Minor comments:

Line 107: The sentence may be revised for clarity.

See reply to Major Comment 2

Line 180-181: Provide reference?

This is determined by our own calculations based on the difference of the mean O2 absorption cross sections in channels A and B defined in the manuscript and constraints on column density of O2 along the line of sight. After revisiting these calculations, the O2 affect is much smaller than the stated 1.5%. The percent difference in the mean O2 absorption cross section between the two channels is 1.5%. This corresponds to an even smaller difference in transmittance given the low column density of O2 between the emission region and instrument.

Text in Section 3.2 has been updated as follows (Lines 176-180):

"Sources of representativeness error in deriving T_{ci} are those that cause relative differences in the channel intensity other than temperature that are not captured in the vibrational-rotational band model. Photoabsorption by O_2 is one source to consider. There is only a 1.5% difference in the mean absorption cross section between the two channels that corresponds to a negligible difference in transmittance due to O_2 along the line-of-sight considering the O_2 absorption cross section variation with temperature."

Line 242: Full disk measurements goes on until 23 UTC.

This mistake is updated in the revised manuscript (Line 238).

Line 288: What is the x-axis in figure 7? Is it local time at all longitudes or local times at fixed longitude?

The x-axis is the date/time in UT. It is not in local time. The zonal mean is computed considering all longitudes over the disk for a particular GOLD scan.

Reviewer 2 response:

Specific comments

1. **Line 90 – Is the factor of 1.6 mentioned here an issue with the current approach? My understanding form later sections is that it is not. If this is the case, I believe it would be worth explicitly stating that here.**

   The factor of 1.6 is not an issue with the current approach. This is only true because we have recently started using the vibrational population rates provided in Ajello et al. (2020) that were determined from GOLD data instead of the theoretical Franck Condon factors as stated in line 96. However, there are uncertainties around the vibrational population rates in Ajello et al. (2020) which adds another error source that is discussed in the response to Comment 2. Section 2.1 is updated such that the discussion on the excitation and extinction source is being removed and the focus is on the band model as follows (Lines 79-91):

   "The forward model used to produce synthetic LBH emissions is built with the Global Airglow Model (GLOW) and a radiative transfer model (Solomon, 2017). GLOW computes LBH volume emission rates as a function of altitude that are input into the radiative transfer model to produce line-of-sight emissions of the LBH band system. The most important component of the forward model for the purposes of deriving thermospheric temperatures is the LBH vibrational-rotational band model (Budzien et al., 2001). The band model is a look-up table of laboratory spectra that specifies, for a given temperature, a unique spectrum for the upper vibrational states v′=0–9 of N_2. In the current implementation of the forward model, the v′=0–9 vibrational population rates are those provided in Ajello et al. (2020) that are based on GOLD observations and are held constant. The population rate distribution can vary with the energy distribution of the electron flux in addition to variation in excitation sources other than direct excitation such as radiative cascade and collision-induced electronic transition (Ajello et al., 2020, Eastes et al., 2000a,b; Ajello et al., 1985). Ajello et al. (1985) states that excitation thresholding should be included in airglow models to accurately reproduce LBH band intensity. However, as discussed in the following section, absolute band intensity is not needed to extract the N_2 rotational temperature."

2. **Line 177 – Is this statement true, if the model for LBH with temperature is imperfect?**

   Thank you for pointing this out. No, this statement would not be true if the model for LBH with temperature is imperfect. The model for LBH with temperature is the rotational-vibrational band model. The greatest source of imperfection to this model is the specification of the v′=0-9 population rates. The manuscript in various sections is updated and a new figure is added to Section 3.2 to quantify this error as follows:

Abstract – line 12: "The two-channel ratio approach limits representativeness and measurement error by only requiring measurement of the relative magnitudes between two spectral channels and not radiometrically calibrated intensities, simplifying the forward model from a full radiative transfer model to only a vibrational-rotational band model."

Section 3.2 – line 177: deleted

Section 3.2 – line 176-192: "Sources of representativeness error in deriving T_{ci} are those that cause relative differences in the channel intensity other than temperature that are not captured in the vibrational-rotational band model. Photoabsorption by O_2 is one source to consider. There is only a 1.5% difference in the mean absorption cross section between the two channels that corresponds to a negligible difference in transmittance due to O_2 along the line-of-sight considering the O_2 absorption cross section variation with temperature. Another source of representativeness error associated with the (2,0) band is due to the overlap of the bright (2,0) transition and the weak (5,2) transition. Inaccurate specification of the v′=2 and v′=5 vibrational population rates cause a slight change in shape of the band with respect to the observations that could be interpreted as a change in the rotational temperature. Figure 8 in Ajello et al. (2020) provides the v′=0–6 population rates and their uncertainties. These uncertainties are used to determine the associated error in the derived temperatures using the (2,0) band due to inaccurate specification of the v′=2 and v′=5 population rates. It is important to note that this representativeness error does not exist if the (1,1) or (2,3) bands are used in the derivation instead of the (2,0) band because the (1,1) and (2,3) bands are isolated from other LBH bands. However, these bands are also much weaker and suffer from significantly larger random error due to shot noise. Figure 4 shows the total random measurement error and representativeness error in T_{ci} using the (2,0) band. The representativeness error is a function of temperature and can range from 15 K at T_{ci} = 400 K to 48 K at T_{ci} = 1200 K. Random measurement error from shot noise is a function of the (2,0) band intensity with values of 20 and 50 K for a photon counts of 2500 and 500, respectively."

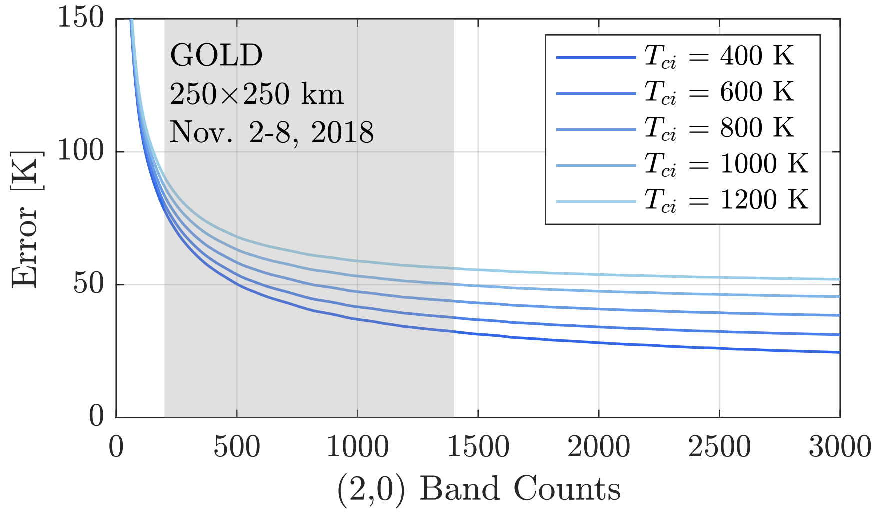

Figure 4: Total random measurement error (not including particle noise) and representativeness error for T_{ci} using the (2,0) band. The range of (2,0) band counts for GOLD data (250 ×250 km resolution at nadir) used in the case study in Section 4 is highlighted by the grey box.

Section 5 – line 329: "*In this two-channel ratio approach, representativeness errors originating from forward modeling are reduced because radiometrically calibrated LBH band intensities are not required in the derivation procedure, and negative impact of systematic measurement errors, stemming from variations across the band system in the instrument's wavelength registration and resolution, are reduced because a fully resolved LBH band system is not required.*"

3. **Line 180 – I believe that the O_2 absorption cross-section also varies (albeit not strongly) as a function of temperature. This will further complicate this factor, although it is likely still minor.**

   The O_2 absorption cross section does vary with temperature, however, this temperature dependence does not change the relative absorption between the two channels. The main text is updated as follows (lines 178-180):

   "There is only a 1.5% difference in the mean absorption cross section between the two channels that corresponds to a negligible difference in transmittance due to O_2 along the line of sight considering the O_2 absorption cross section variation with temperature."

4. **Line 182 – It is certainly true that the shot noise, which is proportional to the square root of the emission signal, is a major part of the instrumental noise. However, particle noise is, at least at some times, an additional**

random noise source. Importantly, it's behavior is not the same as the shot noise as it is unrelated to the brightness of the signal being observed. See for example the description of the particle background and its associated flag in GOLD Release Notes Revision 4 - https://gold.cs.ucf.edu/wp-content/documentation/GOLD_Release_Notes_Rev4.1.pdf. This may, potentially, be an important consideration in the case study presented in this manuscript.

We agree with the reviewer. The need to consider particle noise as another random noise source is a strong point. We have reviewed the particle background counts and its associated flag for observations used in the case study and found relatively low counts (~0-0.3) with the high background flag set to false. Therefore, we do not think the particle background counts affect the results of this manuscript, but it will be important moving forward to (1) quantify the statistics of background counts as a function of wavelength and (2) quantify the associated temperature errors. The following text is included in Section 3.2 (Lines 171-175):

"Particle background counts is at times an additional random noise source. For the case study with GOLD data, the particle backgrounds were low as indicated by the "High_Background" flag in the Level 1C data and therefore this error source is not considered. The statistics of background counts and the associated temperature errors should be quantified for the general application of this technique to any period."

Line 267 – The east-west gradient that is described here is not clear to me in Figure 5. I would recommend that this be demonstrated more clearly, perhaps in a line-figure such as Figure 6, as I believe it is an important point that current, at least I struggle to see from the image.

To address the reviewer's concern, Figure 6 (shown below) has been updated such that the RMSD plot has been removed and replaced with the MBD as a function of longitude. Note that the comparison between T^{G}_{ci} and T_MSIS changed because the MSIS temperatures are updated based on new sampling with respect to both OZA and SZA (see response to Reviewer 1 Major Comment 6). Also, note that since the comparison has been updated with T_DISK version 3, the interpretation of Figure 5 and Figure 6 (now Figure 7 and Figure 8) has changed but the major conclusions from the manuscript remain unchanged. The east-west gradient is more pronounced now in the TDISK product similar to that in T^{G}_{ci} although the T^{G}_{ci} is still more pronounced as seen in the updated Figure 6 (now Figure 8) below. These interpretations are updated in the manuscript on lines 266-275.

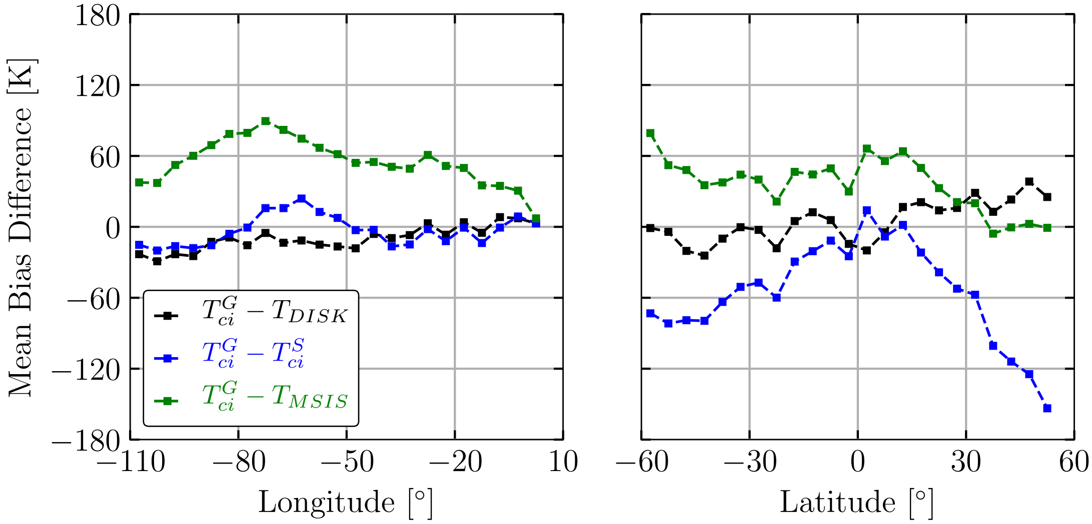

Figure 8: Mean bias difference (MBD) of T^G_{ci} from T_{DISK}, T_{MSIS}, and T^S_{ci} for 5° bins as a function of longitude (left) and latitude (right) during 2–8 November 2018 at 15 UT. All longitudes viewed by GOLD are considered when computing MBD as a function of latitude and only equatorial latitudes between ±10° are considered when computing MBD as a function of longitude.

5. **Figure 5 – The range over the disk where T_ci_G appear is smaller than that of Tdisk. Is the origin of this a differences in the solar zenith angle ranges, or some other criteria used in the approach described here that differs from the publicly available Tdisk?**

   Figure 5 is now Figure 7. There was an error in the plotting routine that masked more T^G_{ci} compared to TDISK as a function of solar and observing zenith angle. This error has been corrected and each of the temperature products is plotted over the same range of observing zenith angle and solar zenith angle as shown in the updated Figure 7 (see Figure 7 in response to Reviewer 1 Major Comment 6).